

**Developmental Cell, Volume 44**

**Supplemental Information**

**Innate Immune Response and Off-Target Mis-splicing**

**Are Common Morpholino-Induced Side Effects**

**in *Xenopus***

**George E. Gentsch, Thomas Spruce, Rita S. Monteiro, Nick D.L. Owens, Stephen R. Martin, and James C. Smith**

## Legends for Supplemental Figures

### Figure S1. Generation of the Double Heterozygous Line for *Brachyury* paralogues *t* and *t2*, Related to Figure 1

(A) Scheme to generate the  $t^{e1.2D/+}t2^{e3.7D/+}$  ( $t^{+/+}t2^{-/+}$ ) *X. tropicalis* line. (B,F) TALEN design for *t* or *t2* mutagenesis and positions of MOs blocking donor splice site (MO<sub>splice</sub>) or translation initiation site (MO<sub>transl</sub>) of the corresponding transcript. (C,G) TALEN-induced mutation rate at the targeted *SacI* or *EcoRI* site as estimated by the partial restriction digest of specific PCR amplicons. (D) Sanger sequencing summary of generated indels in exon 1 of *t*. (E) Morphological defects caused by TALEN-induced *t* mutations at late tailbud stage. Scale bar, 0.5 mm. (H) Western blot of injected wild-type and mutant *t* or *t2* constructs tagged either N- or C-terminally with *HA*. The detection of exogenous myc (as part of the injected *fam83g-myc* mRNA) and endogenous  $\alpha$ -tubulin were used as controls for injection/translation efficiency and gel electrophoresis loading, respectively. (I) Mutant *Brachyury* constructs failed to disrupt gastrulation. Scale bar, 0.25 mm.

### Figure S2. *Brachyury* KO and KD Embryos Are Morphologically Very Similar, Related to Figure 2

(A) Gross morphological comparison between different conditions of the KD and KO experiment at the indicated tailbud stages. Uninjected (uni) and control MO (cMO)-injected embryos were controls for the *t/t2* morphants (*t/t2* MO). Wild-type (wt) embryos were siblings of the mutant embryos (hetero- and homozygous for the mutant *t* and *t2* allele, *t/t2* het and *t/t2* KO). Scale bar, 0.5 mm. (B) Comparison of low fragment count gene transcripts to estimate minimal fragment count required for calling reliable fold changes. Genes that averaged <7 fragments between cMO-injected and uninjected and heterozygous and wild-type embryos over tailbud stage 26 and 34 were excluded due to a higher degree of spurious fold changes.

### Figure S3. Increased Transcription of *tp53* Depending on GC Content of MO Does Not Cause More Apoptosis, Related to Figure 3 and 4

(A) TUNEL assay on morphants and sibling embryos from double heterozygous  $t^{+/+}t2^{+/-}$  parents. DNase-treated wild-type embryos were used as positive controls. (B) Single WMISH for *tp53* and multi-probe WMISH for various mesoderm cell lineage and

derivative markers (*cav1*, notochord; *hoxd8*, pronephros; *myh6*, heart; *tal1*, ventral blood island; *tbx6*, paraxial mesoderm) of late tailbud embryos injected with single MOs or tracer sulforhodamine-dextran. Scale bar, 0.5 mm.

**Figure S4. Specific MOs of the *t/t2* MO Cocktail Cause Off-Target Splicing Defects, Related to Figure 5**

(A,C) Superimposed Sashimi plot of *abi1* and *bloc1s4* transcripts whose splicing was perturbed by the injected *t/t2* MO mix. Canonical and alternative splicing are shown with solid and dashed lines, respectively. Blocked splice sites containing matches of  $\geq 8$  consecutive bases with a specific MO are shown as alignments. Canonical Watson-Crick and non-canonical wobble base pairing are marked as vertical bar and colon, respectively. (B,D) RT-qPCR ( $n = 4$ , mean  $\pm$  SD) confirmed that specific MOs of the *t/t2* MO mix were responsible for mis-splicing. The fold change ( $\log_2$  scale) of transcript levels and alternative splicing between exon 7 and 11 (*abi1*) and exon 4 and 6 (*bloc1s4*) are shown as filled and solid bars, respectively. Two-tailed t-test: \*,  $p \leq 0.1$ ; \*\*,  $p \leq 0.01$ . See Figure 3D and Key Resources Table for the design of RT-qPCR primers.

**Figure S5. Temperature and MO Dosage Effects on *Brachyury* Phenotype and Immune Response Related Gene Transcription, Related to Figure 7**

(A) WMISH for *tp53* of late tailbud embryos injected with 4.5 or 18 ng of the *t/t2* MO mix and developed at 22 °C or 28.5°C. \*, Remark: Increasing incubation temperature also slightly up-regulated *tp53* in the absence of any MO (confirmed by RT-qPCR, data not shown). (B) Multi-probe WMISH for various mesoderm cell lineage and derivative markers (*cav1*, notochord; *hoxd8*, pronephros; *myh6*, heart; *tal1*, ventral blood island; *tbx6*, paraxial mesoderm) and single WMISH for *tp53*, *tp53inp1* and *c3ar1* of mid-tailbud (stage 26) and late tailbud embryos (stage 34) injected with 6 or 18 ng of the *t/t2* MO mix. White arrowheads point to the expression domains of *tbx6* and *cav1* that were not maintained in embryos without functional *Brachyury*. (C) WMISH for *tp53inp1* on wild-type (or *t/t2* heterozygous) and *t/t2* null mutant embryos as well as embryos injected with 1 and 3 ng MO. The embryos were developed to late tailbud stage 34 at 25-26°C. Scale bar, 0.5 mm.

Figure S1

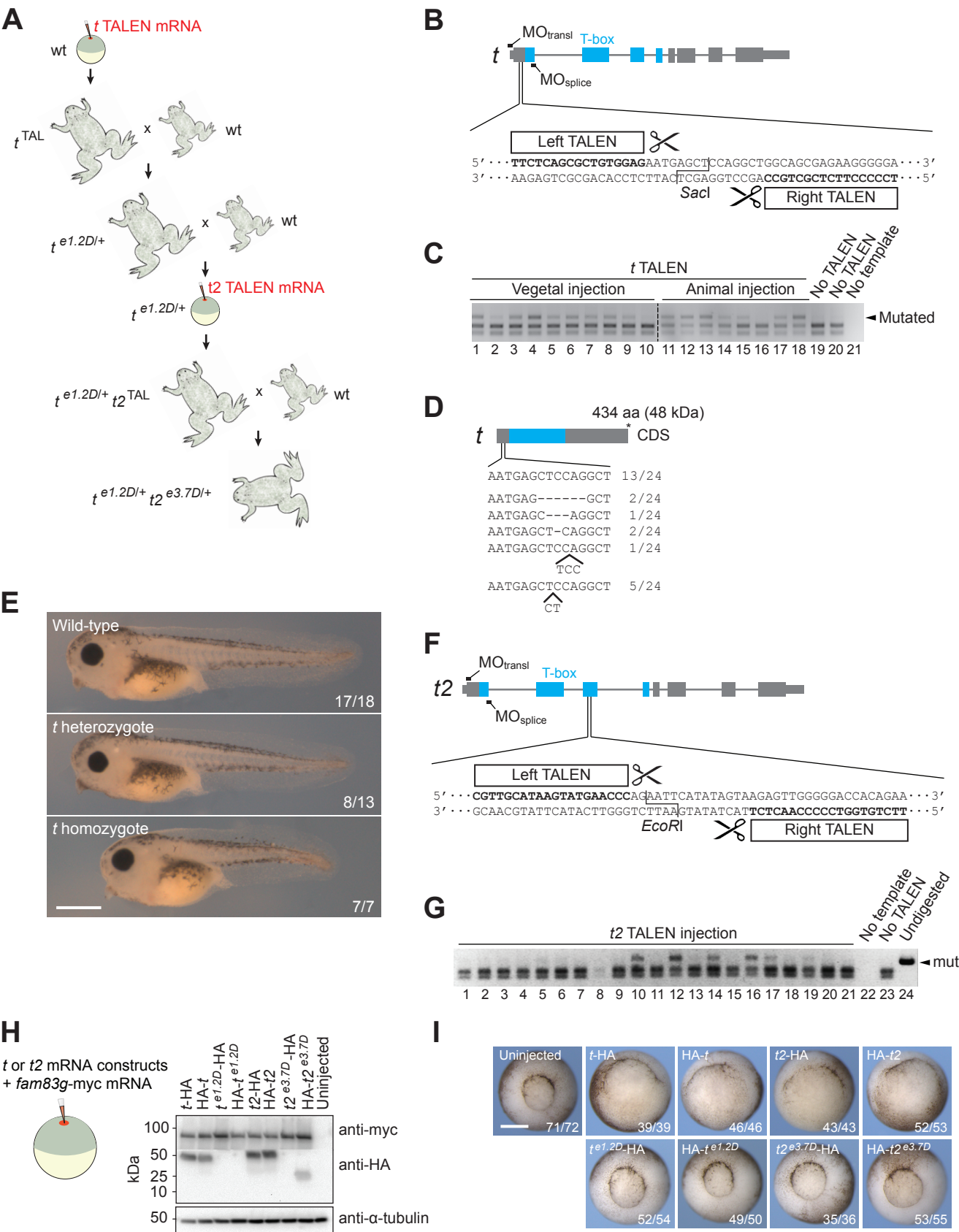
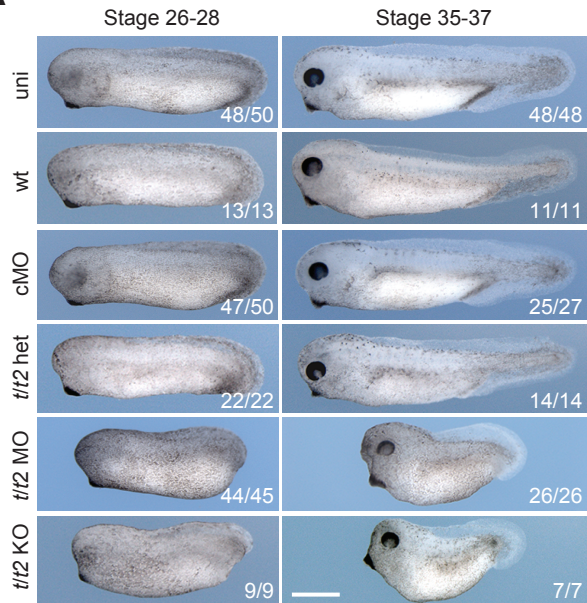
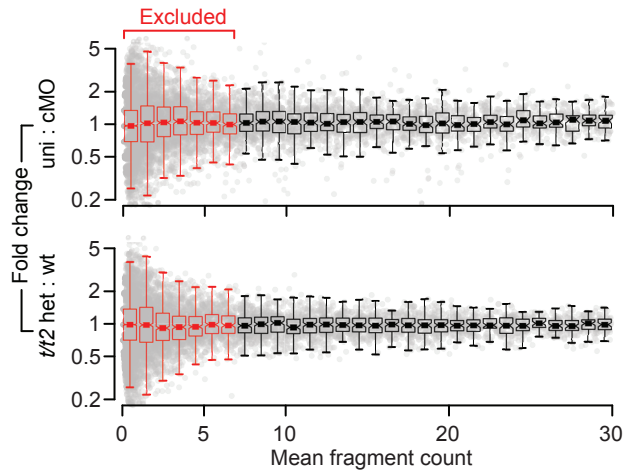


Figure S2

**A**



**B**

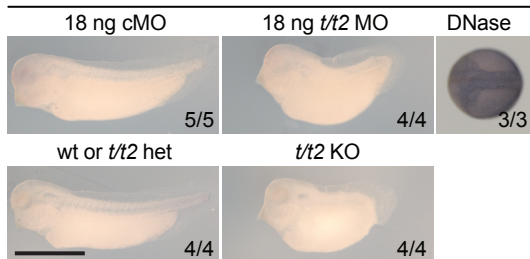


# Figure S3

## A

Late tailbud stage 34

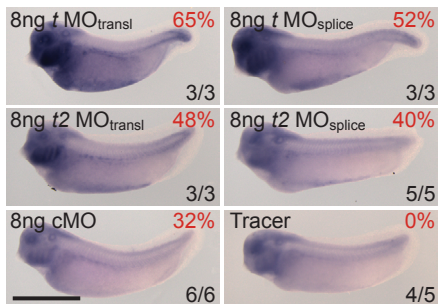
TUNEL



## B

Late tailbud stage 34

GC % of MO sequence vs. *tp53* induction



Mesoderm marker expression in *t* and *t2* morphants

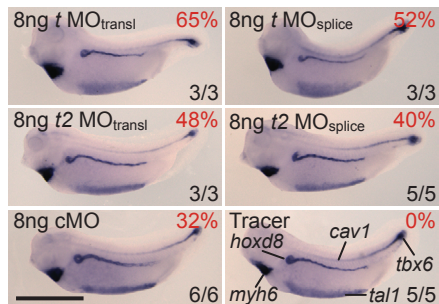
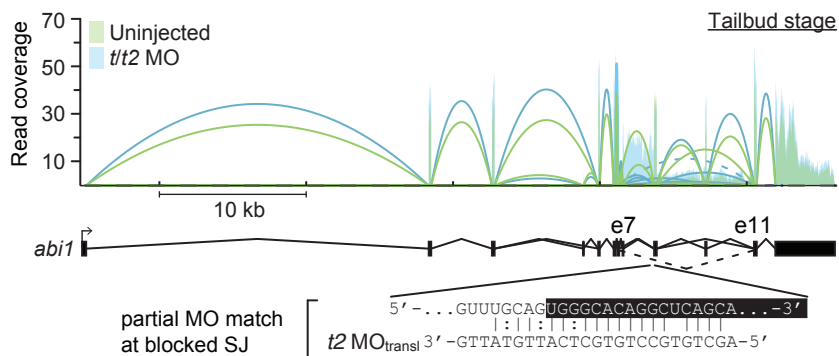


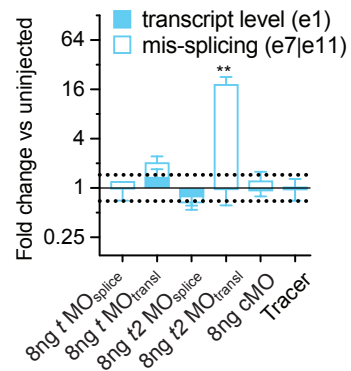
Figure S4

**A**

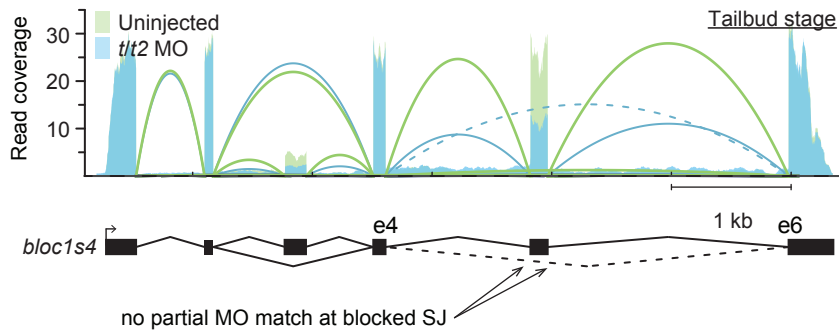


**B**

*abi1* at late tailbud stage



**C**



**D**

*bloc1s4* at late tailbud stage

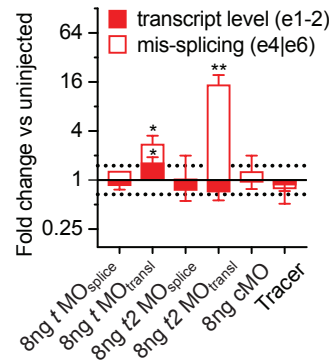
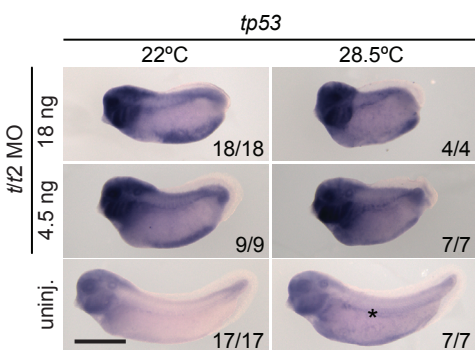


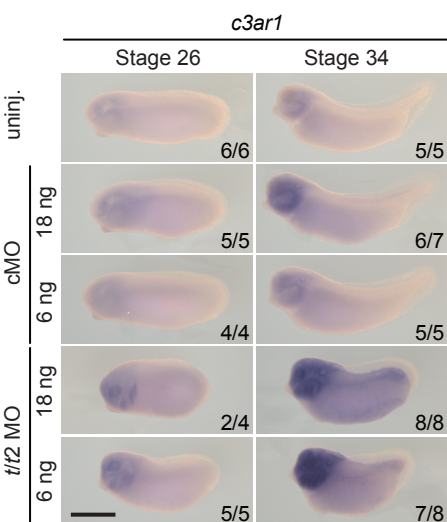
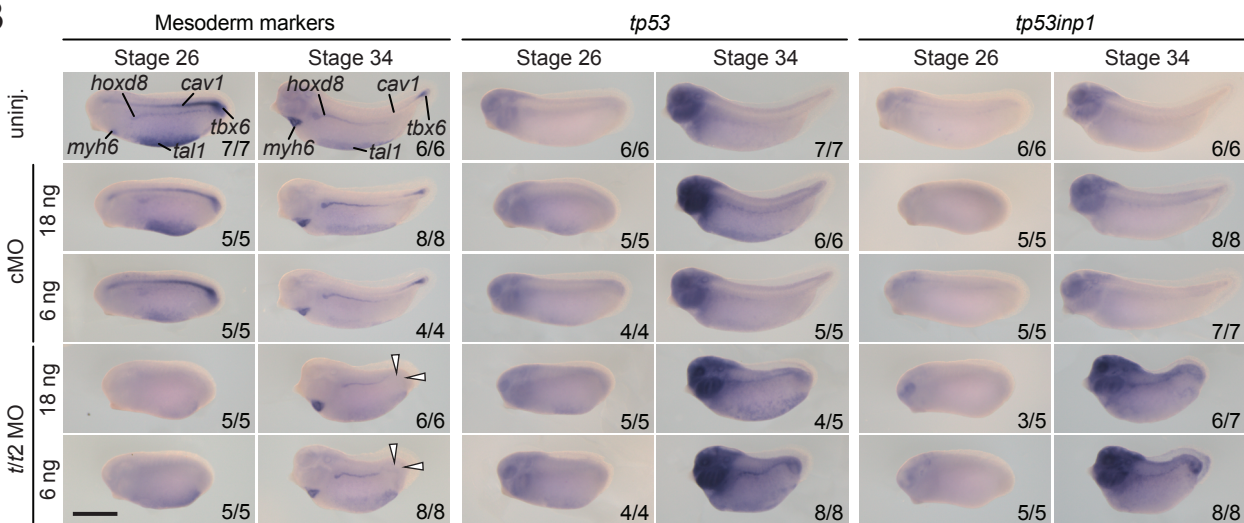
Figure S5

**A**

Late tailbud embryos (stage 34)



**B**



**C**

Late tailbud embryos developed at 25-26°C

